Available online at www.sciencedirect.com
ScienceDirect
Physics of the Earth and Planetary Interiors 160 (2007) 51–59
PHYSICS OF THE EARTH AND PLANETARY INTERIORS
www.elsevier.com/locate/pepi

Making sound inferences from geomagnetic sounding

Ashley E. Medin*, Robert L. Parker, Steven Constable

Green Institute of Geophysics and Planetary Physics, Scripps Institution of Oceanography, University of California at San Diego, 9500 Gilman Drive, La Jolla, CA 92093-0225, USA

Received 14 March 2006; received in revised form 31 August 2006; accepted 8 September 2006

Abstract

We examine the nonlinear inverse problem of electromagnetic induction to recover electrical conductivity. As this is an ill-posed problem based on inaccurate data, there is a critical need to find the reliable features of the models of electrical conductivity. We present a method for obtaining bounds on Earth's average conductivity that all conductivity profiles must obey. Our method is based completely on optimization theory for an all-at-once approach to inverting frequency-domain electromagnetic data. The forward modeling equations are constraints in an optimization problem solving for the electric fields and the conductivity simultaneously. There is no regularization required to solve the problem. The computational framework easily allows additional inequality constraints to be imposed, allowing us to further narrow the bounds. We draw conclusions from a global geomagnetic depth sounding data set and compare with laboratory results, inferring temperature and water content through published Boltzmann–Arrhenius conductivity models. If the upper mantle is assumed to be volatile free we find it has an average temperature of 1409–1539 °C. For the top 1000 km of the lower mantle, we find an average temperature of 1849–2008 °C. These are in agreement with generally accepted mantle temperatures. Our conclusions about water content of the transition zone disagree with previous research. With our bounds on conductivity, we calculate a transition zone consisting entirely of Wadsleyite has < 0.27 wt.% water and as we add in a fraction of Ringwoodite, the upper bound on water content decreases proportionally. This water content is less than the 0.4 wt.% water required for melt or pooling at the 410 km seismic discontinuity.
Published by Elsevier B.V.

Keywords: Geophysical inverse theory; Geomagnetic induction; Electrical conductivity of the mantle; Water in the mantle

1. Introduction

The problem of learning about electrical conductivity of the deep interior of the Earth from time series of the magnetic field at the surface falls in the province of inverse theory. Because of incompleteness and uncertainty, deficiencies shared by all practical measurements, the information contained in data can never furnish a precise description of the conductivity distribution, and so an essential part of any inversion must be an assessment of the variety of possible solutions. The earliest systematic attempt to provide such a measure was the analysis of resolution given by Backus and Gilbert (1968, 1970), applied by Parker (1970) to the question of the global geomagnetic sounding. Backus–Gilbert theory is fundamentally a linear theory, and if the inverse problem is nonlinear, as it is for all electrical problems in geophysics, the equations are linearized on the assumption that any deviation from a base model can be treated as a linear perturbation. While this is a plausible approximation for many seismological applications, the huge range of electrical conductivities encountered even near the surface, from 4 S m^{-1} in surface seawater to 10^{-5} S m^{-1} in igneous rocks (Telford et al., 1990), casts doubt on its

* Corresponding author. Tel.: +1 858 822 5996; fax: +1 858 534 5332.
E-mail address: amedin@ucsd.edu (A.E. Medin).

0031-9201/$ – see front matter Published by Elsevier B.V.
doi:10.1016/j.pepi.2006.09.001

trustworthiness for electrical problems. Furthermore, another characteristic of the electromagnetic forward problem invalidates linear resolution theory: a thin perfect conductor (one with infinite conductivity) introduced into a model can cause only a finite, perhaps even a tiny, change in the measured responses, whereas the linear theory predicts an infinite response to an infinite perturbation. Consequently in the inverse problem, small differences in the observations may be associated with arbitrarily large model variations which the linear approximation critically underestimates, a serious flaw in a method for assessing model reliability (Parker, 1982).

In the usual analysis of magnetotelluric and geomagnetic data (e.g., Constable, 1993; Olsen, 1999) the range of solutions is explored by constructing regularized models under a variety of penalty functions, with particular emphasis on the solutions with minimum complexity as measured by the norm of its gradients. A much more informative approach to the question of model ambiguity is to identify an interesting property of the model, and to use optimization methods to find its maximum and minimum values which then supply bounds on the quantity of interest. Oldenburg (1983) introduced this idea and applied it the electromagnetic inverse problem concentrating on the property of conductivity averages. The same strategy has been successfully applied in a number of linear inverse problems, in which other model properties have been bounded (Stark et al., 1986; Parker, 1991, 2003; Parker and Song, 2005). A key consideration in these linear problems has been the way in which inequality constraints have played a role in obtaining useful conclusions; for example, positivity of the unknown or its gradient. In this paper we will present a method for obtaining bounds in the nonlinear electromagnetic inverse problem in a way that permits the natural introduction of inequality constraints into the computational framework. The extension of computational techniques to cover the nonlinear and nonconvex optimization problems that arise will be the subject of the first part of the paper.

There are two complementary ways in which we can learn about the deep interior: the first is inversion of observations made at the surface, and the second is by studying the properties of likely materials in the laboratory. In the case of electrical conductivity, there is broad agreement between the results of the two strategies (e.g., Constable, 1993; Xu et al., 1998), but whether that agreement is adequate or not must depend on the uncertainty ascribed to the conductivity models, something known only poorly, if at all. We propose to provide a credible assessment of those uncertainties.

2. Inversion by homogeneous optimization

For the purposes of this study we will need to consider only the one-dimensional magnetotelluric (MT) inverse problem, a problem described many times before (e.g., Weidelt, 1972; Whittall and Oldenburg, 1992; Parker, 1994). Weidelt (1972) showed that the inverse problem in a spherically symmetric Earth can be mapped exactly into a one-dimensional MT problem of the following kind. We treat a conducting layer in $0 \le z \le H$ with positive z downard, above which there is a horizontal magnetic field varying as $e^{i\omega t}$; the electrical conductivity σ is a function of z alone. Observations are made of perpendicular horizontal electric and magnetic fields at $z = 0$, which permit the estimation of $c(\omega)$, a complex admittance given by

$$c(\omega) = \frac{E(0,\omega)}{i\omega B(0,\omega)} = -\frac{E(0,\omega)}{E'(0,\omega)} \tag{1}$$

where $E(z,\omega)$ is the y component of the (complex) electric field at depth z, $B(z,\omega)$ is the x component of the magnetic induction, and prime denotes the z derivative. For $z > 0$ the electric field obeys the differential equation

$$E''(z,\omega) = i\omega\mu_0\sigma(z)E(z,\omega) \tag{2}$$

which we will solve subject to the boundary conditions

$$E'(0,\omega) = -1, \qquad E(H,\omega) = 0 \tag{3}$$

Here $z = H$ corresponds to the position of a lower boundary where a perfect conductor is situated; in practice for our problem this is the top of the core. With these boundary conditions, we see from (1) that $c(\omega) = E(0,\omega)$. From measurements of time series, the admittance in (1) can be estimated at N frequencies $\omega_1, \omega_2, \ldots, \omega_N$, and so there are N versions of (2), one for each frequency. In the broadest terms, the inverse problem consists of finding out as much as possible about the function $\sigma(z)$ from the N complex numbers $c_j = c(\omega_j)$; it must be understood that these values are not known exactly, but are associated with uncertainties, usually characterized by standard deviations found from spectral analysis of the original time series (e.g., Egbert and Booker, 1986).

To make progress with the inversion we need a measure of misfit between the predictions of a candidate conductivity model and observed admittances: traditionally this has been based on the square of a weighted misfit

$$X[\sigma]^2 = \sum_{j=1}^{N} \frac{|c_j - E(0,\omega_j)|^2}{\epsilon_j^2} \tag{4}$$

where ϵ_j is the standard error of the j-th admittance, assumed here to be the same number for the real and imaginary parts of c_j. If the errors in c_j are Gaussian, then X^2 will be distrbuted as χ^2_{2N} because each frequency contributes two degrees of freedom. The exact minimizer of X^2 (Parker, 1980; Parker and Whaler, 1981) consists of the sum of series of delta functions in conductivity, and so the best-fitting profile (the D^+ solution) is not a geophysically plausible model. To discover smoother, and therefore more acceptable solutions, one might minimize instead

$$P[\sigma] = X[\sigma]^2 + \lambda \|\mathrm{d}\sigma/\mathrm{d}z\|^2 \tag{5}$$

where $\|\cdot\|$ is the L_2 norm (Parker, 1994), and λ is a positive weight chosen so that the solution achieves an acceptably small value of X^2, typically about $2N$. This is regularization. Other regularizations replace the conductivity with its log, use second derivatives, or include a multiplicative weight $w(z)$ in the norm used for regularization (e.g., Constable, 1993).

To minimize the functional P a model $\sigma(z)$ is guessed, (2) is solved numerically, and the gradient of P with respect to changes in σ is calculated on the basis of a linear perturbation analysis, which gives

$$c_j[\sigma + \Delta\sigma] = c_j[\sigma] + \langle D_j, \Delta\sigma\rangle + o\|\Delta\sigma\| \tag{6}$$

where $\Delta\sigma(z)$ is a perturbing function, $\langle\cdot,\cdot\rangle$ is an inner product, D_j is the Frechet derivative of the admittance, which is a function on the interval $(0, H)$; see Parker (1994). Expressed in a finite-dimensional approximation, the inner product is just a matrix multiplication with a dense matrix $D \in \mathbb{R}^{2N\times L}$ where L is the number of parameters used to represent the function $\sigma(z)$. The derivatives, D_j, and hence the corresponding matrix, D, can be written in terms of $E(z, \omega_j)$, the solutions to (2). The gradient of P with respect to σ is easily found from D, and then (5) can be minimized iteratively using conjugate gradients (Rodi and Mackie, 2001) or some other scheme (Constable et al., 1987).

Models found by regularization may suggest the presence of features in the Earth, but by themselves give no useful information about the variety of alternative models. To provide an answer to this question we propose a computational approach that relies on constrained optimization. Instead of employing the two-phase strategy sketched above which alternates between solving the forward problem and perturbing the conductivity, we treat the complex electric fields at each frequency as unknowns, in addition to the conductivity, in a large *constrained* optimization system. Suppose for the sake of concreteness we propose to minimize the function

$$R[\sigma] = \left\| \frac{\mathrm{d}\sigma}{\mathrm{d}z} \right\|^2 \tag{7}$$

the first-derivative roughness of the solution. We apply as equality constraints the differential equations

$$E_j''(z) - \mathrm{i}\omega_j\mu_0\sigma(z)E_j(z) = 0, \quad j = 1, 2, \ldots, N \tag{8}$$

where $E_j(z) = E(z, \omega_j)$; we include as constraints the boundary conditions

$$E_j'(0) = -1; \qquad E_j(H) = 0, \quad j = 1, 2, \ldots, N \tag{9}$$

Furthermore we impose the linear inequality constraint:

$$\sigma(z) \geq 0 \tag{10}$$

Finally, we state that the solution must match the data adequately by means of a nonlinear inequality constraint

$$\sum_{j=1}^{N} \frac{|c_j - E_j(0)|^2}{\epsilon_j^2} \leq T^2 \tag{11}$$

where T is a tolerance set so that the stipulated misfit would occur only rarely by chance. Large-scale optimization in which the electric fields at all points within the model, and at all observed frequencies, are included as unknowns along with the conductivity, has been introduced to solve two- and three-dimensional regularized inversions of electrical problems by Haber et al. (2000, 2004); they call this an "all-at-once" approach.

The calculations (8)–(10) will be applied to an L-vector in the finite-dimensional approximation. The optimization system set out by Eqs. (7)–(11) becomes practical computationally only if we exploit the fact that the differential operator in (8) is represented by a sparse matrix, one that can be stored with order L values for each frequency rather than L^2. Furthermore, aside from the nonlinearity in (11), the only nonlinear term here is the multiplication of σ and E_j in (8), which makes exact calculation of the gradients easy and fast.

The minimization of R in (7) solves a regularized inversion, but our objective is different: we wish to place definite limits on more informative properties of the model than the norm of its gradient. For example, to ascertain how small the average conductivity can be in part of the mantle, say in the depth interval (z_0, z_1) km, we would minimize

$$\bar{\sigma} = \frac{1}{z_1 - z_0} \int_{z_0}^{z_1} \sigma(z)\,\mathrm{d}z \tag{12}$$

subject to the constraints (8)–(11). In fact with the algorithm we have used, it is computationally more efficient to replace (11) by (12) as a linear equality constraint for

a series of values of $\bar{\sigma}$, and to minimize X^2 for each one. In this way we generate a trade-off curve between misfit and mean conductivity. The trade-off curve intersects the tolerance level T^2 twice, once at the lower bound on $\bar{\sigma}$ and once at the upper bound. Thus we will solve the problem

$$\min_{\sigma} \sum_{j=1}^{N} \frac{|c_j - E_j(0)|^2}{\epsilon_j^2} \tag{13}$$

subject to (10) and

$$E_j''(z) - \mathrm{i}\omega_j \mu_0 \sigma(z) E_j(z) = 0 \tag{14}$$

$$E_j'(0) = -1 \tag{15}$$

$$E_j(H) = 0 \tag{16}$$

$$\frac{1}{z_1 - z_0} \int_{z_0}^{z_1} \sigma(z)\,\mathrm{d}z = \bar{\sigma} \tag{17}$$

Notice that the positivity condition (10) is vital in this problem, for otherwise negative conductivities would almost certainly arise. The use of the $\log \sigma$ to insure positivity, a tactic often used to avoid an explicit inequality constraint, is unsuitable because if the optimal conductvity vanishes anywhere (as we find it often does) the log becomes unbounded.

The actual computational scheme we have employed is a general optimizing program called SNOPT (Gill et al., 2002, 2005a,b), which is based on sequential quadratic programming (SQP) and iterative methodology which we will outline here. SQP finds the minimizer of an objective function $f_0(x) : \mathbb{R}^n \to \mathbb{R}$ subject to linear and nonlinear constraints, through a series of iterations. The general optimization problem to be solved is

$$\begin{aligned} &\min_{x,s} && f_0(x) \\ &\text{subject to} && l_x \le x \le u_x \text{ and } l \le g(x) \le u \end{aligned} \tag{18}$$

where $g(x) : \mathbb{R}^n \to \mathbb{R}^m$ is a vector-valued, possibly nonlinear function. Since linear inequality constraints are easier to handle, we introduce a vector slack variables, new unknowns, which convert (18) into a problem with linear inequality constraints and a set of nonlinear equality constraints

$$\begin{aligned} &\min_{x,s} && f_0(x) \\ &\text{subject to} && l_x \le x \le u_x, l \le s \le u \text{ and } g(x) - s = 0 \end{aligned} \tag{19}$$

To enforce (19) we introduce a vector of Lagrange multipliers π, and the Lagrangian $\mathcal{L}$ by

$$\mathcal{L}(x, \pi) = f_0(x) - \pi^{\mathrm{T}}(g(x) - s) \tag{20}$$

By elementary theory x^*, the stationary points of $\mathcal{L}$, that is, where $\nabla\mathcal{L}(x^*, \pi^*) = 0$, correspond to stationary points of f_0 but the linear inequality conditions are not yet satisfied. The solution to the problem is supplied by the Karush–Kuhn–Tucker theorem (Gill et al., 1981), which states that the minimization of $\mathcal{L}$ must be over the subspace of vectors orthogonal to the gradients of the constraints.

The approach to SQP is to solve a series of subproblems with $k = 1, 2, \ldots$ called major iterations; at each such step, a quadratic program problem is set up that approximates the original problem based on the current best solution vector x_k, s_k and the multiplier vector π_k. The modified Lagrangian is

$$\begin{aligned} \mathcal{L}_k(x, x_k, \pi_k) = {} & f_0(x) - \pi_k^{\mathrm{T}}(g(x) - g(x_k) \\ & - g'(x_k)(x - x_k)) \end{aligned} \tag{21}$$

in which the constant and linear part of $g(x)$ in the original $\mathcal{L}$ have been removed. A quadratic approximation to the original problem is now set up as

$$\begin{aligned} \min_{x,\pi,s} \quad & f_0(x_k) + (x - x_k)^{\mathrm{T}} \nabla f_0(x_k) \\ & + \tfrac{1}{2}(x - x_k)^{\mathrm{T}} H_k (x - x_k) \end{aligned} \tag{22}$$

$$\begin{aligned} \text{subject to} \quad & l_x \le x \le u_x, l \le s \le u \text{ and } g(x_k) \\ & + g'(x_k)(x - x_k) - s = 0 \end{aligned} \tag{23}$$

where H_k is a approximation to $\nabla\nabla\mathcal{L}_k$. Notice that the constraints (23), both inequalities and equality, are all linear, so that (22) and (23) is a standard quadratic programming (QP) problem, which is solved iteratively. The solution of the QP problem, $\hat{x}_k$, $\hat{\pi}_k$, $\hat{s}_k$, is not usually a good point to start the next major iteration, because the approximations may be not good enough when x_k is far from x^*. So the next point is chosen by performing a line search on the linear interpolation joining x_k, π_k, s_k to $\hat{x}_k$, $\hat{\pi}_k$, $\hat{s}_k$, seeking the point that reduces f_0 sufficiently to initiate the next major iteration.

The SQP method sketched above and realized practically in SNOPT has been applied to (13)–(17) and (10), and after application of SQP, Weidelt's transformation is done to account for spherical geometry. Finally, we note that the choice of the function to minimize in (12) is surprisingly restricted if informative results about averages are to be discovered. For example, one might seek to minimize the average of log conductivity in an interval, which seems natural given the large range of conductivity values found in Earth materials. However, there is no finite lower bound on the function, because a thin layer of zero conductivity would drive the mean value of log conductivity to negative infinity, yet such a layer would,

if thin enough, have negligible effect on the admittances. The same argument applies to averages of resistivity.

3. Results from global sounding data sets

Because we are considering the one-dimensional MT inverse problem, we desire data that represent average radial structure over large areas. Two data sets that have this property are from Constable (1993) and Olsen (1999). Constable provides a 15 complex point set compiled from land observatories around the globe. Olsen compiles a set of 23 complex points from land observatories in Europe only, but over a much larger frequency range than Constable used. We would like to invert a combination of these data sets so our conclusions can be as strong as possible. However, we need to make sure we are inverting a data set that is indeed representative of one-dimensional structure. We use the D^+ solution discussed earlier as a guide for selecting a one-dimensional data set by checking that the exact minimizer of $X^2 \approx 2N$ (Parker, 1980; Parker and Whaler, 1981). The combined set of all 38 admittances has a D^+ solution with X^2 too large. The most significant contributors to the large X^2 are the longest and shortest period admittances from the set Constable compiled, and the 6-month period and 10-day period admittance from the set Olsen compiled. We remove these four admittances from the combined data set on the following justifications in respective order.

(1) As discussed by Petersons and Constable (1996), as the period gets longer in the data from Constable, the P_0^1 source-field assumption used in the calculation of the admittance breaks down. Olsen does not make a P_0^1 source-field assumption in his long period data.
(2) The shorter period data explore shallower structure. Presumably shallower structure has more global variation than deeper structure so the European bias from the data complied by Olsen would be expected to represent a one-dimensional structure that differs from the average global one-dimensional structure. We choose to keep the short period data from the European compilation and remove the global shortest period datum to make the sets compatible. An analysis of daily variation was used in the collection of the short period European admittances making them more reliable than those relying on the P_0^1 assumption. We accept the risk that we may be biasing the shallow inversion results towards Europe.
(3) Olsen himself excludes the 6-month period admittance from his analysis of his European compilation since the assumption about the relative noise-to-signal ratio he made may fail at that period.

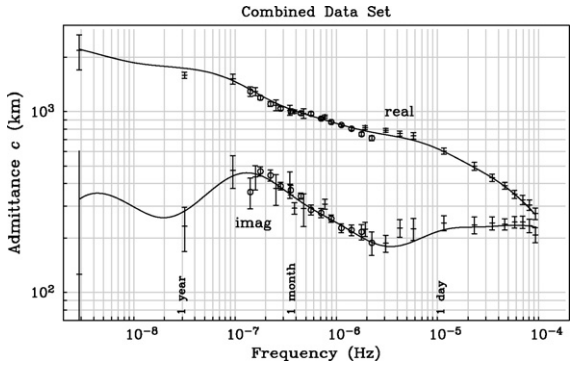

Fig. 1. Complex conjugates of admittances used in inversion along with error bars. Note that the error bar for the longest period imaginary admittance runs off of the plot. The data from Constable (1993) are plotted as circles and the data from Olsen (1999) as horizontal bars. The lines are the D^+ solution.

(4) The only surprising part of the D^+ solution on the combined 38 admittance set was the large contribution of the 10-day period datum from Olsen to the overall X^2. This datum has an error bar half the size of those of the surrounding data. Since we have no basis for adjusting the error, we removed this data point.

The combined 34 admittance set is plotted in Fig. 1 along with the D^+ solution. The D^+ solution puts a perfect conductor at 2430.5 km, which corresponds to the top of the core after Weidelt's spherical transformation. The minimum X^2 is 72, reasonable for a one-dimensional data set of this size.

We perform the optimization with the combined data set and find bounds on $\bar{\sigma}$ of (12) over parts of the mantle. Interesting parts of the mantle are the upper mantle (0, 410) km, the transition zone (410, 670) km, and the top 1000 km of the lower mantle (670, 1670) km. Sensing the bottom of the lower mantle is problematic because very long time-series of the magnetic fields are needed and furthermore it is difficult to properly remove the secular variation prior to the estimation of the admittance functions. Thus we prefer to limit our results to the top of the lower mantle. We assume the errors in c_j are Gaussian and choose the tolerance level T^2 of Eq. (11) to be the 90% left-tail probability, i.e. level, of the χ^2_{2N} distribution. We solve for $\sigma(z_k)$ at discrete points $k = 1, 2, \ldots, K$, as this is a numerical optimization problem. The optimization was done with $K = 21$, $K = 31$, and $K = 61$; no significant difference in the bounds resulted. The reported bounds have $K = 31$. Because the discrete points are evenly spaced in the chosen computational framework, the actual regions of the mantle are (0, 418), (418, 672), and (672, 1666) km. The

Table 1
90% χ^2 level bounds on the average value of conductivity, $\bar{\sigma}$

Added constraints	$\bar{\sigma}$ in (S m^{-1}) for depth interval in (km)		
	[0, 418]	[418, 672]	[672, 1666]
None[a]	$0.002 \leq \bar{\sigma} \leq 0.025$	$0.020 \leq \bar{\sigma} \leq 0.276$	$1.09 \leq \bar{\sigma} \leq 2.76$
Monotonicity[b]	$0.013 \leq \bar{\sigma} \leq 0.017$	$0.120 \leq \bar{\sigma} \leq 0.193$	$1.61 \leq \bar{\sigma} \leq 2.10$

[a] Conductivity allowed to increase and decrease with depth.
[b] Conductivity allowed to only increase with depth.

resulting bounds on $\bar{\sigma}$ over the three parts of the mantle are given in Table 1.

These bounds are not based on regularization but cover all possible conductivity profiles, including highly oscillatory ones. Technically, we have tested the hypothesis that the greatest value of the mean conductivity in the suite of all models consistent with the data falls below the stated bound; the test is performed at the 90% probability level. The lower bound is obtained in a similar way. The interval between the bounds does not correspond to the standard 90% confidence interval for average conductivity as we have not made a statistical estimate of average conductivity itself. Although the bounds are fairly restrictive, we can narrow them further if we are willing to make additional assumptions. To the first-order, conductivity is a thermally activated Boltzmann process of the form

$$\sigma = \sigma_0 \mathrm{e}^{-A/kT} \tag{24}$$

for a constant σ_0, activation energy A, Boltzmann's constant k, and temperature T. Thus it is commonly accepted that conductivity increases monotonically with depth due to increasing temperature, or

$$\frac{\mathrm{d}\sigma}{\mathrm{d}z} \geq 0 \tag{25}$$

We add (25) as a constraint to our previous optimization problem (13)–(17), and achieve more restrictive bounds on $\bar{\sigma}$ reflected in Table 1.

We show the bounds in Fig. 2. The gray boxes are the ranges of average conductivity without constraining (25), monotonicity of σ. The black boxes are the restricted ranges with monotonicity. We stress that the regions delineated in Fig. 2 are not error bars for a particular model of conductivity; they indicate the permitted range in average conductivity of every possible model that fits the sounding data. We now proceed to draw conclusions about mantle properties from these bounds.

4. Mantle temperature

The conductivity of likely materials of the mantle has been studied extensively in the laboratory. These experiments give us empirical equations relating the conductivity of the material to its temperature. Clearly the conclusions we draw will only be as reliable as the laboratory results but we must start somewhere.

We first look at the upper mantle. The mineralogy of the upper mantle is dominated by olivine. The next most abundant mineral is clinopyroxene, which has a conductivity–temperature relationship similar to that of olivine and so models of upper mantle conductivity are often based on olivine. We used the SEO3 model for the olivine temperature–conductivity relationship (Constable, 2006). SEO3 is based on a Boltzmann model of defect mobilities and concentrations obtained from relatively low-temperature conductivity and thermopower measurements on a natural, silica-buffered, rock, thus avoiding the alteration that often occurs during high-temperature laboratory measurements of conductivity. See Constable (2006) for the equations. Recent measurements on single crystal olivine by Du Frane et al. (2005) have a much lower apparent activation energy, and would result in much higher temperature bounds. The Du Frane et al. paper serves to illustrate the difficulty

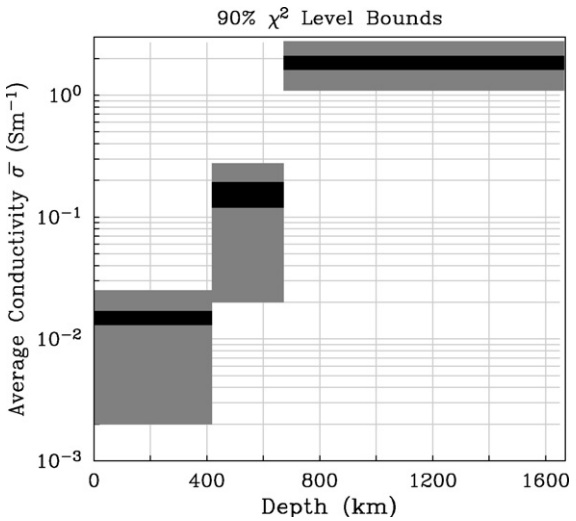

Fig. 2. Bounds on average conductivity. The gray boxes are the ranges without constraining monotonicity of σ; the black are the restricted ranges with monotonicity.

that still exists in obtaining representative laboratory data sets, as well as the gaps that remain in our understanding of electrical conduction mechanisms, even in well-studied minerals such as olivine. Until these gaps are filled, our use of SEO3 is based on a preference for data originating from poly-phase, poly-crystalline samples, and the thermodynamic model behind the temperature extrapolation.

Using the SEO3 model for a mantle at an oxygen fugacity determined by the quartz–fayalite–magnetite buffer, our monotonic bounds of $0.013 \leq \bar{\sigma} \leq 0.017\,\mathrm{S\,m^{-1}}$ predict an average temperature of 1409–1430 °C, in excellent agreement with conventional estimates of an adiabatic mantle temperature (Schubert et al., 2001). The temperature bounds are highly dependent on the conductivity model chosen, and even other parameters such as mantle oxygen fugacity. For example, using our bounds the SEO3 model predicts an average temperature range of 1515–1539 °C for mantle with an iron-wüstite buffer. However, all calculated ranges are too close to the conventionally accepted temperatures to support the idea of a significant conductivity associated with volatile content in the upper mantle (e.g., Karato, 1990).

We perform a similar comparison with the laboratory research on the likely conductors of the lower mantle. The conductivity of the lower mantle is most likely governed by silicate perovskite containing 4 to 5% Al_2O_3 by weight (Xu et al., 1998). Although the lower mantle is 20% magnesiowüstite by volume, the perovskite phase is thought to be not insulating enough and the magnesiowüstite not interconnected enough for magnesiowüstite to contribute significantly to the conductivity structure of the lower mantle (Martinez et al., 1997; Xu et al., 1998). Xu et al. propose the following model of the aluminum-bearing perovskite conductivity

$$\sigma\,(\mathrm{S\,m^{-1}}) = 74\,\mathrm{e}^{-0.70\,\mathrm{eV}/kT} \tag{26}$$

We calculate the average temperature of the top 1000 km of the lower mantle as we did with the entirety of the upper mantle. We assume monotonic growth of σ with depth so that $1.61 \leq \bar{\sigma} \leq 2.10\,\mathrm{S\,m^{-1}}$. Then with (26) we constrain the average temperature of the top of the lower mantle to be be 1849–2008 °C, within the range obtained by considering the adiabatic gradient (Schubert et al., 2001). If the magnesiowüstite is considered interconnected, the calculated average temperature would be implausibly low since magnesiowüstite is much more conductive than aluminum-bearing perovskite (Dobson and Brodholt, 2000).

5. Water content of the transition zone

High pressure phases of olivine control the conductivity of the transition zone. Olivine deforms into its β-phase, Wadsleyite, at 410 km and its γ-phase, Ringwoodite, at 520 km. These minerals have a much higher water solubility than that of the upper and lower mantle minerals, and Bercovici and Karato suggested in 2003that the transition zone may act as a water reservoir. Furthermore, they proposed that the water content of the transition zone may exceed the critical concentration so that water pools and creates partial melt at the 410 km seismic discontinuity. Melt here would have a large effect on the geochemical cycling in Earth. The critical concentration of water would be reached if the transition zone had more water than the storage capacity of the upper mantle. This storage capacity was originally inferred by Kohlstedt et al. (1996) as 0.16 wt.% water. However, recently Hirschmann et al. (2005) suggest that Kohlstedt et al. underestimated the water concentration in olivine by their use of the Paterson method (Paterson, 1982) and give a revised minimum capacity of 0.4 wt.%. So, do our conductivity bounds support a water content of more than 0.4 wt.% in the transition zone?

Huang et al. (2005) give an empirical conductivity model of the transition zone as a function of water content and temperature based on the equation

$$\sigma_{\mathrm{Wad,Lab}}\,(\mathrm{S\,m^{-1}}) = 380\,C^{0.66}\,\mathrm{e}^{-0.91\,\mathrm{eV}/kT} \tag{27}$$

for Wadsleyite, and

$$\sigma_{\mathrm{Ring,Lab}}\,(\mathrm{S\,m^{-1}}) = 4070\,C^{0.69}\,\mathrm{e}^{-1.08\,\mathrm{eV}/kT} \tag{28}$$

for Ringwoodite, where σ_{Lab} is the conductivity estimated in the laboratory and C is water content by weight percent. Finally they set $\sigma_{\mathrm{Earth}} \approx 0.5\sigma_{\mathrm{Lab}}$ to correct laboratory oxygen fugacity to Earth oxygen fugacity. Notice that for a given C, $\sigma_{\mathrm{Ring}} > \sigma_{\mathrm{Wad}}$, supporting monotonic growth of σ for a transition zone with Ringwoodite occurring deeper than Wadsleyite.

We take a rough average of our calculated upper and lower mantle temperatures to get a typical transition zone temperature of 1600 °C. Huang et al. assume a similar temperature and also note that temperature has a small effect on conductivity relative to the effect of water. We then use our calculated bounds on conductivity to find the possible range of average water content in the transition zone. Again assuming monotonic growth of conductivity with depth, we have the transition zone bounds $0.120 \leq \bar{\sigma} \leq 0.193\,\mathrm{S\,m^{-1}}$. These give us 0.08–0.15 wt.% average water content if the transition zone was composed entirely of Wadsleyite, and

0.01–0.02 wt.% if it was only Ringwoodite. However, if we do have melt then monotonicity will not hold locally around 410 km and our upper bound on the transition zone average conductivity must change to 0.276 S m^{-1}, or 0.27 wt.% water for an all Wadsleyite composition (0.04 wt.% water for all Ringwoodite). These are simple pessimistic end-member models which allow us to calculate water content bounds independent of the complications of mixing laws, mineral fractions, and properties of other minerals in the transition zone. As stated earlier, the transition zone is believed to be over half Ringwoodite. Thus our monotonic conductivity bounds support a water content of $\ll 0.4$ wt.%, suggesting that there will not be melt or water pooling at the 410 km seismic discontinuity.

6. Conclusions

We have used an optimization method to recover radially averaged conductivity from geomagnetic sounding data, a nonlinear inverse problem. The optimization method allowed us to find bounds on the average conductivity over parts of the mantle, and to add constraints to tighten these bounds. We did not use regularization. We then used these bounds to draw conclusions about the temperature and water content of the mantle through empirical relations measured in the laboratory. Our conclusions clearly are dependent on the fidelity of the laboratory measurements.

Our upper mantle bounds along with the laboratory conductivity model of dry olivine constrain the average temperature to be 1409–1539 °C, which is close to conventionally accepted temperatures. If the mantle oxygen fugacity is known this range can be tightened further. In any case, our work supports an almost volatile-free upper mantle. The lower mantle calculations are based on laboratory conductivity studies of perovskite with aluminum. Here our conductivity bounds constrain the average temperature of the top 1000 km of the lower mantle as 1849–2008 °C, again agreeing with conventional values. Using an assumed average temperature of 1600 °C in the transition zone, our bounds constrain an absolute upper limit on average water content of the transition zone of 0.27, or 0.15 wt.% for a monotonic conductivity profile. This is for a completely Wadsleyite transition zone; as Ringwoodite is added to the composition the upper limit decreases fractionally. We conclude that the transition zone is unlikely to have melt or water pooling at the 410 km seismic discontinuity as a global feature. As our conductivity bounds are radial averages, local melt or pooling is possible as long as the net conductivity is balanced elsewhere.

The code used in generating average conductivity bounds from any given set of admittances is available at http://igppweb.ucsd.edu/~parker/software.htm.

Acknowledgements

We thank Philip Gill and Joshua Griffin for providing SNOPT and assisting with its use. The work of Ashley Medin was supported by the Scripps Institution of Oceanography Seafloor Electromagnetic Methods Consortium. The work of Steven Constable was supported by NASA under NAG5-13747. Suggestions by two anonymous reviewers led to improvements in the manuscript.

References

Backus, G.E., Gilbert, J.F., 1968. The resolving power of gross Earth data. Geophys. J. R. Astr. Soc 16, 169–205.

Backus, G.E., Gilbert, J.F., 1970. Uniqueness in the inversion of inaccurate gross Earth data. Phil. Trans. R. Soc. Lond. A 266, 187–269.

Bercovici, D., Karato, S.I., 2003. Whole-mantle convection and the transition-zone water filter. Nature 425 (6953), 39–44.

Constable, S., 1993. Constraints on mantle electrical conductivity from field and laboratory measurements. J. Geomag. Geoelectr. 45, 707–709.

Constable, S., 2006. SEO3: a new model of olivine electrical conductivity. Geophys. J. Int. 166 (1), 435–437.

Constable, S., Parker, R.L., Constable, C.G., 1987. Occam's inversion: apractical algorithm for generating smooth models from electromagnetic sounding data. Geophys. 52, 289–300.

Dobson, D.P., Brodholt, J.P., 2000. The electrical conductivity of the lower mantle phase magnesiowüstite at high temperatures and pressures. J. Geophys. Res. 105 (B1), 531–538.

Du Frane, W.L., Roberts, J.J., Toffelmier, D.A., Tyburczy, J.A., 2005. Anisotropy of electrical conductivity in dry olivine. Geophys. Res. Lett. 32, L24315.

Egbert, G.D., Booker, J.R., 1986. Robust estimation of geomagnetic transfer-functions. Geophys. J. Roy Astron. Soc. 87, 173–194.

Gill, P.E., Murray, W., Saunders, M.A., 2005a. User's guide for SNOPT 7.1: a Fortran package for large-scale nonlinear programming. Technical Report NA 05–2, Department of Mathematics, University of California at San Diego.

Gill, P.E., Murray, W., Saunders, M.A., 2005b. SNOPT: an SQP algorithm for large-scale constrained optimisation. SIAM Review 47, 99–113.

Gill, P.E., Murray, W., Wright, M.H., 1981. Practical Optimization. Academic Press, New York.

Haber, E., Ascher, U.M., Oldenburg, D.W., 2000. On optimization techniques for solving nonlinear inverse problems. Inverse Prob. 16 (5), 1263–1280.

Haber, E., Ascher, U.M., Oldenburg, D.W., 2004. Inversion of 3D electromagnetic data in frequency and time domain using an inexact all-at-once approach. Geophysics 69, 1216–1228.

Hirschmann, M.M., Aubaud, C., Withers, A.C., 2005. Storage capacity of H_2O in nominally anhydrous minerals in the upper mantle. Earth Planet. Sci. Lett. 236, 167–181.

Huang, X.G., Xu, Y.S., Karato, S.I., 2005. Water content in the transition zone from electrical conductivity of wadsleyite and ringwoodite. Nature 434 (703), 746–749.

Karato, S., 1990. The role of hydrogen in the electrical conductivity of the upper mantle. Nature 347, 272–273.

Kohlstedt, D.L., Keppler, H., Rubie, D.C., 1996. The solubility of water in α, β, and γ phases of $(Mg, Fe)_2 SiO_4$). Contrib. Miner. Petrol. 123, 345–357.

Martinez, I., Wang, Y.B., Guyot, F., Liebermann, R.C., Doukhan, J.C., 1997. Microstructure and iron partitioning in $(Mg, Fe)_2 SiO_3$) perovskite (Mg, Fe)O magnesiowüstite assemblages: An analytical transmission electron microscopy study. J. Geophys. Res. 102, 5265–5280.

Oldenburg, D.W., 1983. Funnel functions in linear and nonlinear appraisal. J. Geophys. Res. 88 (NB9), 7387–7398.

Olsen, N., 1999. Long-period (30 days–1 year) electromagnetic sounding and the electrical conductivity of the lower mantle beneath Europe. Geophys. J. Int. 138 (1), 179–187.

Parker, R.L., 1970. The inverse problem of electrical conductivity in the mantle. Geophys. J. R. Astr. Soc. 22, 121–138.

Parker, R.L., 1980. The inverse problem of electromagnetic induction: existence and construction of solutions based upon incomplete data. J. Geophys. Res. 85, 4421–4428.

Parker, R.L., 1982. The existence of a region inaccessible to magnetotelluric sounding. Geophys. J. R. Astr. Soc. 68, 165–170.

Parker, R.L., 1991. A theory of ideal bodies for seamount magnetism. J. Geophys. Res. 96 (B10), 16101–16116.

Parker, R.L., 1994. Geophysical Inverse Theory. Princeton University Press, Princeton.

Parker, R.L., 2003. Ideal bodies for Mars magnetics. J. Geophys. Res. 108 (E1), 5006 doi:10.1029/2001JE001760.

Parker, R.L., Song, Y.Q., 2005. Assigning uncertainties in the inversion of NMR relaxation data. J. Magn. Reson. 174 (2), 314–324.

Parker, R.L., Whaler, K., 1981. Numerical methods for establishing solutions to the inverse problem of electromagnetic induction. J. Geophys. Res. 86, 9574–9584.

Paterson, M.S., 1982. The determination of hydroxyl by infrared absorption in quartz, silicate glasses and similar materials. Bull. Mineral. 105, 20–29.

Petersons, H.F., Constable, S., 1996. Global mapping of the electrically conductive lower mantle. Geophys. Res. Lett. 23 (12), 1461–1464.

Rodi, W., Mackie, R.L., 2001. Nonlinear conjugate gradients algorithm for 2D magnetotelluric inversion. Geophys. 66 (1), 174–187.

Schubert, G., Turcotte, D.L., Olson, P., 2001. Mantle Convection in the Earth and Planets. Cambridge University Press, Cambridge.

Stark, P.B., Parker, R.L., Masters, G., Orcutt, J.A., 1986. Strict bounds on seismic velocity in the spherical earth. J. Geophys. Res. 91 (B14), 13892–13902.

Telford, W.M., Geldart, L.P., Sheriff, R.E., 1990. Applied Geophysics, 2nd ed.. Cambridge University Press, Cambridge.

Weidelt, P., 1972. The inverse problem in geomagnetic induction. Z. Geophys. 38, 257–289.

Whittall, K.P., Oldenburg, D.W., 1992. Inversion of Magnetotelluric Data for a One-dimensional Conductivity. SEG Monograph Series 5.

Xu, Y.S., McCammon, C., Poe, B.T., 1998. The effect of alumina on the electrical conductivity of silicate perovskite. Science 282 (5390), 922–924.